4-1-2024

Sensitive MRD detection from lymphatic fluid after surgery in HPV-associated oropharyngeal cancer

Noah Earland
Washington University School of Medicine in St. Louis
Nicholas P Semenkovich
Washington University School of Medicine in St. Louis
Ricardo J Ramirez
Washington University School of Medicine in St. Louis
Peter K Harris
Washington University School of Medicine in St. Louis
Andrew I Hearn
Washington University School of Medicine in St. Louis

See next page for additional authors

Sensitive MRD Detection from Lymphatic Fluid after Surgery in HPV-Associated Oropharyngeal Cancer

Noah Earland[1,2], Nicholas P. Semenkovich[2,3], Ricardo J. Ramirez[4], Sophie P. Gerndt[5], Peter K. Harris[1], Zhuosheng Gu[6], Andrew I. Hearn[4], Matthew Inkman[1], Jeffrey J. Szymanski[1], Damion Whitfield[6], Benjamin M. Wahle[4], Zhongping Xu[7], Kevin Chen[1], Irfan Alahi[1,8], Gabris Ni[1], Andrew Chen[1], Wendy Winckler[6], Jin Zhang[1,2,9], Aadel A. Chaudhuri[1,2,8,9,10,11], and Jose P. Zevallos[7,12]

ABSTRACT

Purpose: Our goal was to demonstrate that lymphatic drainage fluid (lymph) has improved sensitivity in quantifying postoperative minimal residual disease (MRD) in locally advanced human papillomavirus (HPV)-associated oropharyngeal squamous cell carcinoma (OPSCC) compared with plasma, and leverage this novel biofluid for patient risk stratification.

Experimental Design: We prospectively collected lymph samples from neck drains of 106 patients with HPV (+) OPSCC, along with 67 matched plasma samples, 24 hours after surgery. PCR and next-generation sequencing were used to quantify cancer-associated cell-free HPV (cf-HPV) and tumor-informed variants in lymph and plasma. Next, lymph cf-HPV and variants were compared with TNM stage, extranodal extension (ENE), and composite definitions of high-risk pathology. We then created a machine learning model, informed by lymph MRD and clinicopathologic features, to compare with progression-free survival (PFS).

Results: Postoperative lymph was enriched with cf-HPV compared with plasma ($P < 0.0001$) and correlated with pN2 stage ($P = 0.003$), ENE ($P < 0.0001$), and trial-defined pathologic risk criteria (mean AUC = 0.78). In addition, the lymph mutation number and variant allele frequency were higher in pN2 ENE (+) necks than in pN1 ENE (+) ($P = 0.03$, $P = 0.02$) or pN0-N1 ENE (−) ($P = 0.04$, $P = 0.03$, respectively). The lymph MRD-informed risk model demonstrated inferior PFS in high-risk patients (AUC = 0.96, $P < 0.0001$).

Conclusions: Variant and cf-HPV quantification, performed in 24-hour postoperative lymph samples, reflects single- and multifeature high-risk pathologic criteria. Incorporating lymphatic MRD and clinicopathologic feature analysis can stratify PFS early after surgery in patients with HPV (+) head and neck cancer.

See related commentary by Shannon and Iyer, p. 1223

Introduction

In locally advanced head and neck squamous cell carcinoma (HNSCC), a major goal of curative-intent treatment is to achieve locoregional control. Locally advanced HNSCC can be treated with curative-intent surgery—primary tumor resection and neck dissection—followed by adjuvant radiotherapy (RT) or chemoradiotherapy (CRT), depending on the pathologic risk assessment (1, 2). However, even under favorable pathologic conditions, up to 30% of HNSCC patients experience locoregional recurrence seeded by occult tumor cells (3). Unfortunately, these occult tumor cells are difficult to detect after surgery using medical imaging because of posttreatment inflammation and low cell numbers (4). Emerging liquid biopsies for cancer offer enhanced minimal residual disease (MRD) sensitivity by targeting cancer-specific biomarkers in plasma and other biofluids. During the posttreatment surveillance period, these assays can detect disease recurrence with impressive lead times over imaging (5–7). Some examples of circulating cancer biomarkers include exosomes, circulating tumor cells (CTC), and cell-free DNA (cfDNA; refs. 5, 8).

Among head and neck cancers, human papillomavirus (HPV)-associated oropharyngeal squamous cell carcinoma (OPSCC) is at the forefront of cfDNA-informed treatment personalization (9). Similar to other solid malignancies, posttreatment MRD in HPV (+) OPSCC can be tracked using next-generation sequencing (NGS) assays that target circulating tumor DNA (ctDNA) at variant allele frequencies (VAF) as low as 0.5% (10). HPV (+) MRD can also be tracked using PCR assays targeting cell-free HPV (cf-HPV), with limits of detection (LOD) as low as 10 viral copies (11–15), or assays targeting HPV RNA (+) CTCs (16). Epidemiologically, the incidence of HPV (+) OSPCCs is rapidly increasing (17) in younger patients who typically have favorable prognoses following standard treatment regimens; surgery and RT or

[1]Division of Cancer Biology, Department of Radiation Oncology, Washington University School of Medicine, St. Louis, Missouri. [2]Division of Biology and Biomedical Sciences, Washington University School of Medicine, St. Louis, Missouri. [3]Division of Endocrinology, Metabolism, and Lipid Research, Department of Medicine, Washington University School of Medicine, St. Louis, Missouri. [4]Department of Otolaryngology-Head and Neck Surgery, Washington University School of Medicine, St. Louis, Missouri. [5]Division of Otolaryngology-Head and Neck Surgery, Allegheny Health Network, Pittsburgh, Pennsylvania. [6]Droplet Biosciences, Inc., Cambridge, Massachusetts. [7]Department of Otolaryngology-Head and Neck Surgery, University of Pittsburgh Medical Center, Pittsburgh, Pennsylvania. [8]Department of Computer Science and Engineering, Washington University in St. Louis, St. Louis, Missouri. [9]Siteman Cancer Center, Washington University School of Medicine, St. Louis, Missouri. [10]Department of Genetics, Washington University School of Medicine, St. Louis, Missouri. [11]Department of Biomedical Engineering, Washington University in St. Louis, St. Louis, Missouri. [12]Hillman Cancer Center, University of Pittsburgh Medical Center, Pittsburgh, Pennsylvania.

A.A. Chaudhuri and J.P. Zevallos contributed equally as co-senior authors of this article.

Corresponding Authors: Aadel A. Chaudhuri, Division of Cancer Biology, Department of Radiation Oncology, Washington University School of Medicine, 4511 Forest Park Avenue, St. Louis, MO 63108. E-mail: aadel@wustl.edu; and Jose P. Zevallos, Department of Otolaryngology, University of Pittsburgh Medical Center, 203 Lothrop Street, Suite 5000, Pittsburgh, PA 15213. E-mail: zevallosjp@upmc.edu

Clin Cancer Res 2024;30:1409–21

doi: 10.1158/1078-0432.CCR-23-1789

Translational Relevance

Lymphatic fluid is readily accessible via surgical drains, which are routinely inserted after neck dissection in patients undergoing surgery for human papillomavirus (HPV) (+) oropharyngeal cancer. This study is the first to broadly characterize lymphatic cell-free DNA (cfDNA), a novel prognostic biomarker. We showed that cancer-associated cf-HPV burden correlates with advanced nodal pathology, namely pN2 stage and extranodal extension (ENE). In addition, we are the first to interrogate tumor-informed variants in cervical lymph and show that mutational burden and allele frequencies were also correlated with pN2 and ENE. We further developed and cross-validated a machine learning risk model informed by lymphatic minimal residual disease, which showed low-risk patients had favorable outcomes [recurrence-free survival (RFS) = 100%] compared with high-risk patients (RFS = 73%). Overall, cervical lymphatic cfDNA represents a powerful approach for detecting postoperative residual disease, with the potential to personalize adjuvant treatment in patients with HPV (+) head and neck cancer.

surgery and CRT (18). Good outcomes and high treatment-associated morbidities have driven clinicians to use advanced histopathologic features and other clinical factors to identify patients whose adjuvant therapy can be safely de-escalated (19–22). Importantly, leveraging MRD biomarkers, such as ctDNA or cf-HPV, could further personalize therapy de-escalation in patients with surgical HPV (+) OPSCC, similar to early stage colorectal cancer (23). With respect to cf-HPV MRD detection early after surgery, a recent study in patients with OPSCC showed that postoperative plasma failed to detect MRD in 30% of total recurrence cases (13). Thus, we aimed to explore the efficacy of a different biofluid that is more proximal to the sites of disease (24).

To address the unmet clinical need for a more sensitive liquid analyte for HPV (+) OPSCC, we developed a novel cfDNA assay using surgical serosanguinous lymphatic fluid (lymph) accumulating in surgical drains following neck dissection. Compared with peripheral blood plasma, this biofluid is more proximal to the sites of disease (the lymph nodes and the primary oropharyngeal lesion), which we hypothesized would lead to improved MRD sensitivity over plasma. This proximity-enhanced sensitivity has already been suggested in studies using tumor-draining veinous blood and other alternative non-plasma biofluids (25–29). In this study, we compared cf-HPV levels between matched lymph and plasma samples prospectively collected from 106 patients with HPV (+) OPSCC 24 hours after surgery. We then benchmarked lymph cf-HPV against American Joint Committee on Cancer (AJCC) 8th edition TNM stage, extranodal extension (ENE), and high-risk pathologic criteria derived from prior de-escalation clinical trials. We also applied tumor-informed hybrid-capture NGS to compare lymph ctDNA with patient pathology. Finally, we developed a lymph cf-HPV-informed machine learning model of progression-free survival (PFS) in our HPV (+) patients. Herein, we report that cancer-associated cfDNA detected in postoperative lymph drainage reflects MRD, effectively risk-stratifies patients, and is prognostic for cancer recurrence.

Materials and Methods

Ethics approval and patient consent

The study was conducted in accordance with recognized ethical guidelines put forth in the Belmont Report. All patients included in this study provided written informed consent to participate, and all biospecimens were collected under Washington University School of Medicine Institutional Review Board–approved biospecimen collection protocols #201102323, #201907149, and #201903142.

Study design and patient eligibility

We prospectively collected lymph ($n = 200$), blood ($n = 67$), and tumor tissue ($n = 54$) samples from 120 head and neck surgical patients, 106 of whom had HPV-associated OPSCC, as determined by p16 IHC staining (30) or HPV RNA *in situ* hybridization (ISH; ref. 31). Both biofluid types were assayed by qPCR to measure cf-HPV, and NGS was performed on lymph to further assess tumor-informed variants. Paired tumors were also assayed by qPCR to confirm patient HPV subtypes and were included in the NGS experiment to identify mutations for tumor-informed monitoring. cf-HPV and ctDNA variants were quantified in the biofluids and compared with pathology and clinical outcomes (**Fig. 1**). Of note, two of the 10 recurrence cases (both distant) did not have paired postoperative plasma available.

Eligibility criteria for the HPV (+) OPSCC cohort included: (i) ≥ 18 years of age, (ii) newly diagnosed, biopsy-proven OPSCC HPV (+) by p16 IHC or HPV RNA ISH, (iii) patients who underwent surgical resection of primary tumors along with neck dissection, (iv) surgical drain usage postoperatively. The exclusion criteria were: (i) recurrent or distant metastatic disease at the time of surgery, (ii) neoadjuvant therapy of any kind before surgery, (iii) incidental presentation with multiple head and neck cancer types, (iv) inability to establish tumor HPV status with certainty due to conflicting clinical p16 IHC and HPV ISH results, (v) postoperative samples that were incorrectly processed.

All adjuvant treatment decisions for the patients involved in this study were made without knowledge of assay results. Treatment began with transoral surgery or transoral robotic surgery (TORS) paired with neck dissection. The oncology team then used standard clinical and pathologic risk criteria to determine adjuvant treatment: RT, CRT, or no adjuvant treatment. External beam RT dose was conventionally fractionated and varied from 42 Gy to 66 Gy; 42 Gy patients were enrolled in the MINT 2 trial at WashU (32).

Patient clinical data capture

All clinical data were obtained from electronic health records of the enrolled patients. Baseline clinical, radiographic, and pathologic features were recorded upon patient enrollment in the study. Subsequent follow-up data, including adjuvant therapy after surgery, treatment outcomes, and dates of disease progression, death, and surveillance follow-up scans, were systematically tracked and collected. Patients' individual pathologic features, extracted from surgical pathology reports, were also combined to classify patients as having either high-, intermediate-, or low-risk pathology according to composite risk definitions described in four recent surgical HPV+ OPSCC clinical trials (Supplementary Table S6, Supplementary Methods; refs. 19–22).

Sample collection, processing, and DNA extraction

All patients underwent Jackson Pratt (JP) surgical drain insertion during surgery. Approximately 24 hours after surgery, lymph drain fluid (lymph) was collected from JP drains in a sterile 50 mL conical tube and transported on ice for processing. In addition, 43 lymph samples were serially collected from 11 patients at 0, 6, 12, 18, and 24 hours after surgery. The de-identified lymph sample was then filtered through a 40-μm cell strainer, EDTA was added to 10 mmol/L, and the solution was centrifuged at 2,000 × *g* for 10 minutes. The supernatant was removed, mixed, and aliquoted in 2 mL microcentrifuge tubes for storage at −80°C. Paired blood samples were

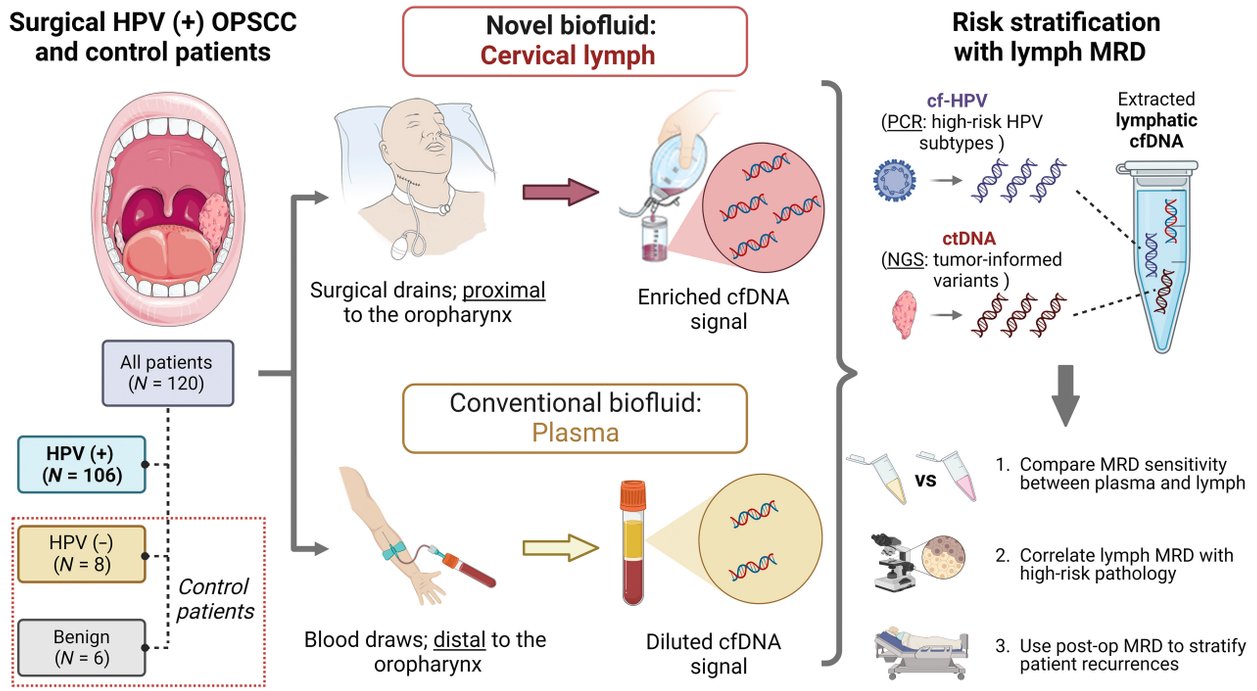

Figure 1.

Schematic of our study design and cohort, which included a total of 120 patients who underwent head and neck surgery for various conditions: HPV (+) OPSCC ($N = 106$), HPV (−) oral cancer ($N = 8$), and benign pathologies of the head and neck ($N = 6$). cfDNA was extracted from 24-hour postoperative lymph and plasma samples. Then, cf-HPV viral load and genotype were determined using PCR, and ctDNA was assessed using tumor-informed variants quantified by hybrid capture NGS. Finally, cf-HPV and ctDNA MRD were compared between plasma and lymph, correlated with pathology, and used to classify cancer recurrence risk. *Note, the cartoon image of the Jackson Pratt drain being emptied into the beaker included in Fig. 1 belongs to Memorial Sloan-Kettering Cancer Center (© 2019: Memorial Sloan-Kettering Cancer Center, Memorial Hospital for Cancer and Allied Diseases, and Sloan-Kettering Institute for Cancer Research, each in New York, NY. All rights reserved. Republished with permission.). MSKCC did not design any other aspects of Fig. 1.*

collected in BD Vacutainer K2 EDTA tubes (BD Biosciences, NJ) at the time of lymph collection. Plasma was prepared by spinning blood first for 10 minutes at 1,200 × *g* and removing the supernatant. We then spun the plasma a second time for 5 minutes at 1,800 × *g*, and the plasma supernatant was removed. The double-spun plasma was then removed, mixed, aliquoted into 2 mL microcentrifuge tubes, and stored at −80°C. Tumor tissue was collected after surgery, snap-frozen in liquid nitrogen, embedded in optimal cutting temperature (OCT) compound blocks on dry ice, and stored at −80°C.

For lymph, we thawed, centrifuged at 1,800 × *g* for 2 minutes, and used 200 µL for cfDNA purification using the QIAamp DNA Mini kit (Qiagen, Germantown, MD) and 100 µL AE buffer elution volume. For plasma, 4 mL was thawed for cfDNA isolation using the Avenio cfDNA Isolation Kit (Roche, Basel, Switzerland). For tumor tissue, we extracted DNA from OCT curls using the QIAamp DNA Mini kit. DNA concentrations were quantified using the Qubit dsDNA Assay (Thermo Fisher Scientific, Waltham, MA) and a Qubit 4 fluorometer (Thermo Fisher Scientific, Waltham, MA).

HPV Taqman PCR assay development

Our cf-HPV Taqman qPCR assay utilized previously described primers and probes targeting HPV16, 18, 31, 33, and 35 (11) and was synthesized by IDT (IDT, Coralville, IA). The qPCR reaction mix consisted of 1 µL HPV primer and probe (2.5 µmol/L), 5 µL 2x PrimeTime Gene Expression Master Mix (IDT, Coralville, IA), 3 µL nuclease-free water, and 1 µL of template DNA. Cycling conditions were 3 minutes at 95°C, 40 cycles × (15 seconds at 95°C and 1 minute at 60°C), then hold at 4°C until storage. The 7900HT Fast Real-time PCR System (Thermo Fisher Scientific, Waltham, MA) was used for qPCR, and cf-HPV copies were quantified using Sequence Detection System (SDS) Software (Thermo Fisher Scientific, Waltham, MA). Three technical replicates were run per sample per assay and up to five independent assays were averaged to determine the cf-HPV copy number per lymph or plasma cfDNA sample. See Supplementary Methods for details regarding digital droplet PCR (ddPCR).

We also established a 95% confidence in our qPCR lower LOD by adapting common standards for qPCR development (33). Briefly, we assayed 24 technical replicates with a 10-fold dilution of the HPV16 E6T2aE7 plasmid in three independent assays (720 assay wells) and determined the minimum dilution at which > 95% of the replicates had detectable HPV (Supplementary Fig. S1D). The TaqMan qPCR LOD was determined to be 10 HPV copies.

Biofluid and tumor NGS

DNA was sequenced from tumor tissue and plasma-depleted whole blood (for germline) using the Novaseq 6000 (Illumina, San Diego, CA). Lymph fluid cfDNA was sequenced using an Illumina NextSeq 2000 (Illumina, San Diego, CA). Tumor and whole-blood genomic DNA (gDNA) were fragmented to approximately 200 bp using Adaptive Focused Acoustics (Covaris, Boston, MA). Bulk lymph cfDNA samples were subjected to ≤ 600 bp fragment selection using a Select-a-Size DNA Kit (Zymo Research, Irvine, CA). The Quant-iT PicoGreen dsDNA assay (Thermo Fisher Scientific, Waltham, MA) and Tapestation (Agilent Technologies, Santa Clara, CA) were used to

assess the quality of the cfDNA and gDNA. Indexed tumor and plasma-depleted whole blood libraries were prepared for whole-exome sequencing using the xGen Exome Hybridization Panel (IDT, Coralville, IA). Indexed lymph cfDNA was prepared and enriched for hotspot target sequences using the TruSight Oncology 500 (Illumina, San Diego, CA) pan-cancer panel (panel size:1.94 MB). Library quality was subsequently assessed using the qPCR NGS Library Quantification Kit (Agilent Technologies, Santa Clara, CA) and Tapestation (Agilent Technologies, Santa Clara, CA). Target coverage was 200x for tumor and germline samples, and 5000x for lymph.

Tumor-informed lymph variant calling

Raw reads for all sample types were demultiplexed and sequencing quality control was performed using Picard CollectHsMetrics version gatk 4.1.7.0 (RRID:SCR_006525). UMI molecular barcode removal and deduplication were completed with Fgbio version 1.1.0 (https://github.com/fulcrumgenomics/fgbio), and reads with paired-end support were aligned to the hg38 human genome using BWA-MEM2 (RRID:SCR_022192) within the nf-core/sarek workflow version 2.7.1 (https://github.com/nf-core/sarek). Lymph samples were then downsampled in triplicate using SAMtools version 1.9 (RRID:SCR_002105) to achieve uniform coverage; tumor samples were not downsampled. Next, mutect2 version gatk 4.1.7.0 (https://gatk.broadinstitute.org/hc/en-us/articles/360037593851-Mutect2) was used to call variants in the tumor tissue and matched germline DNA, extracted from patient-matched PDWB samples, with a depth of coverage threshold >10 and an allelic fraction (AF) threshold of >5%. Any somatic variant with read support in normal PDWB-derived genomic DNA, was filtered out of the total tumor somatic variants called in each patient to prevent variants attributable to clonal hematopoiesis (34) from being called as cancer-associated variants in the lymph or tumor. Then, nonsynonymous mutations (variants resulting in protein sequence changes) were identified using the Ensembl Variant Effect Predictor version 10 (RRID:SCR_007931). The nonsynonymous tumor variants were used to force call mutations in matched lymph samples also using mutect2. Finally, a base-specific error rate was calculated on the basis of the sequencing of lymph ($n = 11$) and plasma samples ($n = 11$) to identify background noise, so nonsynonymous lymph mutations were retained only if they had VAFs greater than this base-specific error rate filter. In addition, in **Figs. 3A** and **B**, when describing nonsynonymous mutations in genes canonically associated with HPV (+) OPSCC, the *canonical* genes were derived from published HPV (+) OPSCC tumor sequencing studies (35–39). In **Fig. 3D**, median VAFs are plotted for each pathology group (pN0-N1, pN1 ENE+, pN2 ENE+).

Generating a prognostic postoperative MRD risk model to stratify disease progression

Our group previously generated a machine learning model that integrates molecular features from a proximal liquid analyte with clinical features to predict PFS (27). To similarly develop a machine learning classifier based on lymph and plasma MRD data, we applied Amazon's AutoGluon-Tabular version 0.8.0 (https://auto.gluon.ai/scoredebugweight/tutorials/tabular_prediction/index.html) and XGBoost to generate a gradient-boosted decision tree (GBDT) model. The model features included lymph cf-HPV copies per mL, plasma cf-HPV copies per mL, age, sex, tobacco pack-years, cancer site, total metastatic nodes, total resected nodes, pathologic T stage, lymphovascular invasion, perineural invasion, ENE, and surgical margin status (Supplementary Fig. S5). XGBoost was run using n_estimators = 10000; learning_rate = 0.1; n_jobs = -1; proc.max_category_levels = 100; objective = binary; logistic; booster = gbtree. The final postoperative MRD risk model performed binary classification (high vs. low risk for relapse). We trained our model using the best_quality AutoGluon preset (which uses a k-fold bagging process to avoid overfitting), targeting an evaluation metric of balanced accuracy, and enabled both automatic sample weighting and decision threshold calibration during training. Model validation was performed via 5-fold internal cross-validation. Feature importance scores were derived via permutation importance as previously described (40).

Statistical and survival analysis

Prism 9.0 (GraphPad Software, San Diego, CA) was used for statistical and survival analyses. We used Fisher exact test to compare the cf-HPV detection rates between plasma and lymph samples. We used the Mann–Whitney U test to compare cf-HPV levels between two patient groups, and the Kruskal–Wallis test to compare cf-HPV levels among more than two groups. We used ROC curves to assess the ability of lymph cf-HPV levels to distinguish high-risk patients from low/intermediate-risk patients, and then calculated the area under the ROC curve (AUC). AUC was also used to evaluate the performance of our postoperative MRD GBDT risk model. Linear correlations were assessed using Spearman's ρ. In the 28 patient NGS cohort, where we compared lymph variants to pathology, we used the robust regression and outlier removal (ROUT) methodology to censor one outlier. Following binary classification by the GBDT model into high- and low-risk patients, PFS was assessed using Kaplan–Meier analysis and the log-rank test. Finally, the reverse Kaplan–Meier method (41) was used to estimate the median follow-up time beginning with the date of surgery.

Data and materials availability

All materials and de-identified data related to this manuscript are available from the corresponding authors upon reasonable request. All bam files corresponding to sequenced patient samples are available from the Sequencing Read Archive under accession number PRJNA1032008 (https://www.ncbi.nlm.nih.gov/bioproject/PRJNA1032008/).

Results

Patient characteristics and cancer control outcomes

From August 2019 to July 2021, 120 surgical patients with HNSCC or benign head and neck conditions were prospectively enrolled. Of these, 106 had HPV (+) disease (**Table 1**; Supplementary Table S1), eight had HPV (-) cancer, and six underwent neck dissection for benign head and neck conditions (Supplementary Table S2; **Fig. 1**). The majority of HPV (+) patients were men (92%) with less than 10-pack-year smoking history (56%), reflecting the expected clinical landscape (18). Most primary tumors were resected from either the tonsils (52%) or base of the tongue (40%), and most (95%) tumors had nonkeratinizing squamous cell carcinoma histology.

Thirty percent of HPV (+) patients received adjuvant CRT, 50% received adjuvant RT, and 20% underwent definitive surgery without adjuvant treatment. The median follow-up time was 24.9 months. Overall, we had four patient deaths and 10 recurrences—four locoregional and six distant metastatic (Supplementary Table S1)—also reflecting expected clinical outcomes (1, 2).

Characterization of lymph cfDNA and postoperative cf-HPV dynamics

In the HPV (+) cohort, 184 total lymph fluid samples were harvested from surgical drains inserted after TORS and neck dissection

Table 1. HPV (+) OPSCC patient characteristics.

Patient characteristics ($n = 106$)	No. (%)
Gender	
Male	97 (91.5)
Female	9 (8.5)
Median age (years)	61
Median follow-up (months)	24.9
Progressed during follow-up	96 (91)
Survived throughout follow-up	102 (96)
Smoking history	
>10 Pack years	47 (44.3)
<10 Pack years	11 (10.4)
Never smoker	48 (45.3)
Primary tumor site	
Tonsil	55 (51.9)
Base of tongue	42 (39.6)
Palatine tonsil	2 (1.9)
Glossotonsillar sulcus	3 (2.8)
Unknown primary tumor	4 (3.8)
Histology	
Nonkeratinizing SCC	95 (89.6)
Other[a]	11 (10.4)
AJCC 8 pathologic T stage	
pT0	6 (5.6)
pT1	48 (45.3)
pT2	48 (45.3)
pT3	2 (1.9)
pT4	2 (1.9)
AJCC 8 pathologic N stage	
pN0	1 (0.9)
pN0*[b]	6 (5.7)
pN1	87 (82.1)
pN1*[b]	82 (77.3)
pN2	18 (17)
ENE	
ENE present	33 (31)
ENE absent	73 (69)
Adjuvant radiotherapy	
66 Gy	5 (4.7)
60 Gy	54 (50.9)
44 Gy	1 (0.9)
42 Gy	24 (22.6)
Unknown dose	1 (0.9)
Received adjuvant radiotherapy or chemoRT[c]	85 (80.2)
Received adjuvant radiotherapy alone	53 (50.0)
Adjuvant chemotherapy	
Yes[d]	32 (30.2)
No	74 (69.8)
No adjuvant treatment	
Definitive surgery alone	21 (19.8)

[a]Other histologic subtypes beside nonkeratinizing SCC included keratinizing SCC, adenosquamous carcinoma, lymphoepithelial carcinoma, basaloid carcinoma, and SCC not otherwise specified.

[b]Seven patients with AJCC 8 stage pN1 disease had excisional lymph node biopsies prior to surgery, where their positive node(s) were removed. In 5 of these patients, no additional nodes were identified at surgery, so they were effectively pN0 when lymph was collected (thus we had 6 pN0* patients, including 1 true pN0 patient). In 2 of the 7 pN1 excisional biopsy patients, additional involved nodes were found at the time of surgery, so they remained stage pN1* when lymph was collected (thus the 87 pN1 patients were reduced to 82 pN1* patients).

[c]Patients that received adjuvant radiotherapy or chemoradiotherapy after surgery.

[d]All adjuvant chemotherapy patients also received concurrent radiotherapy.

along with 67 synchronously collected blood samples (**Fig. 1**). Patients who underwent bilateral neck dissections had two lymph samples banked, and the sample with the highest cf-HPV level was included in our analysis. Seven HPV (+) patients did not meet the inclusion criteria. Overall, 106 HPV (+) lymph samples and 67 plasma samples were included in the final analysis (**Fig. 1**; **Table 1**, Supplementary Table S1). When available, tumor tissue-derived DNA was collected to corroborate the patient's HPV status and determine tumor-informed variants using NGS.

Plasma cfDNA revealed canonical nucleosomal peaks at approximately 180 bp, which were observed in both plasma and lymph cfDNA fragmentomic profiles. Overall, lymph cfDNA displayed a variety of fragment sizes, with relative peaks at 400 and 600 bp, as well as larger molecules likely derived from genomic DNA (Supplementary Fig. S1A). TaqMan qPCR and ddPCR assays were developed to quantify cf-HPV. Because both assays achieved similar performance ($R^2 = 0.98$, $R^2 = 0.99$, respectively), we proceeded with the TaqMan assay, which achieved a LOD of 10 cf-HPV copies (Supplementary Fig. S1B–S1D).

To assess the optimal postoperative lymph collection time, we used the TaqMan assay to quantify cf-HPV in serially collected lymph samples from 11 HPV (+) patients. We observed a sharp decrease in cf-HPV from 0 to 6 hours after surgery, followed by a slower decline from 6 to 24 hours (Supplementary Fig. S1E). At 24 hours, some samples demonstrated a persistent viral signal, whereas others fell below the LOD. To better differentiate these two patterns of cf-HPV levels in lymph, we collected all subsequent biofluids around the 24-hour time-point.

Lymphatic fluid is enriched with cf-HPV and reflects high-risk nodal pathology

First, we compared cf-HPV detection in postoperative plasma and lymph. We observed a wide variation in lymph cf-HPV copy number across the HPV (+) cohort (**Fig. 2A**). Among all HPV (+) lymph ($N = 106$) and plasma ($N = 67$) samples, cf-HPV was detected in 83 lymph samples (78%) compared with eight plasma samples (12%; $P < 0.0001$; **Fig. 2B**). Among paired samples ($N = 67$), the average cf-HPV copies per mL in lymph was more than 9,000-fold higher than the copies per mL in plasma (lymph mean $= 6.05 \times 10^6$ copies/mL, plasma mean $= 6.26 \times 10^2$ copies/mL), which illustrates the magnitude of lymph cf-HPV enrichment relative to plasma ($P < 0.0001$; Supplementary Fig. S4A). Several high-risk HPV subtypes (42) were detected in the postoperative lymph, predominantly HPV16 (74 of 83), but also HPV33 and HPV35 (**Fig. 2B**). As cervical lymphatic drain fluid is a novel liquid analyte, we wanted to assess whether surgical factors had any impact on cf-HPV burden. We observed that the amount of blood contamination in each lymph sample (Supplementary Fig. S2), the specific surgeon who performed TORS (Supplementary Fig. S3A), and the total volume of lymph collected per surgical drain (Supplementary Fig. S3B) had no significant impact on the cf-HPV burden. Finally, no cf-HPV was detected in benign and HPV (-) cancer lymph fluid samples, showing assay specificity for HPV (+) disease (**Fig. 2B**).

Once assay specificity and robustness were confirmed (Supplementary Fig. S1B–S1D), we compared the lymph cf-HPV burden with surgical pathology. We found that cf-HPV copy number was not correlated with primary tumor size (Spearman $\rho = 0.07$; $P = 0.50$; Supplementary Fig. S4B) or AJCC 8th edition pathologic tumor (pT) stage (Kruskal-Wallis, $P = 0.80$; Supplementary Fig. S4C). However, lymph cf-HPV was strongly associated with nodal pathology. First, we found that patients with nodal pathologic

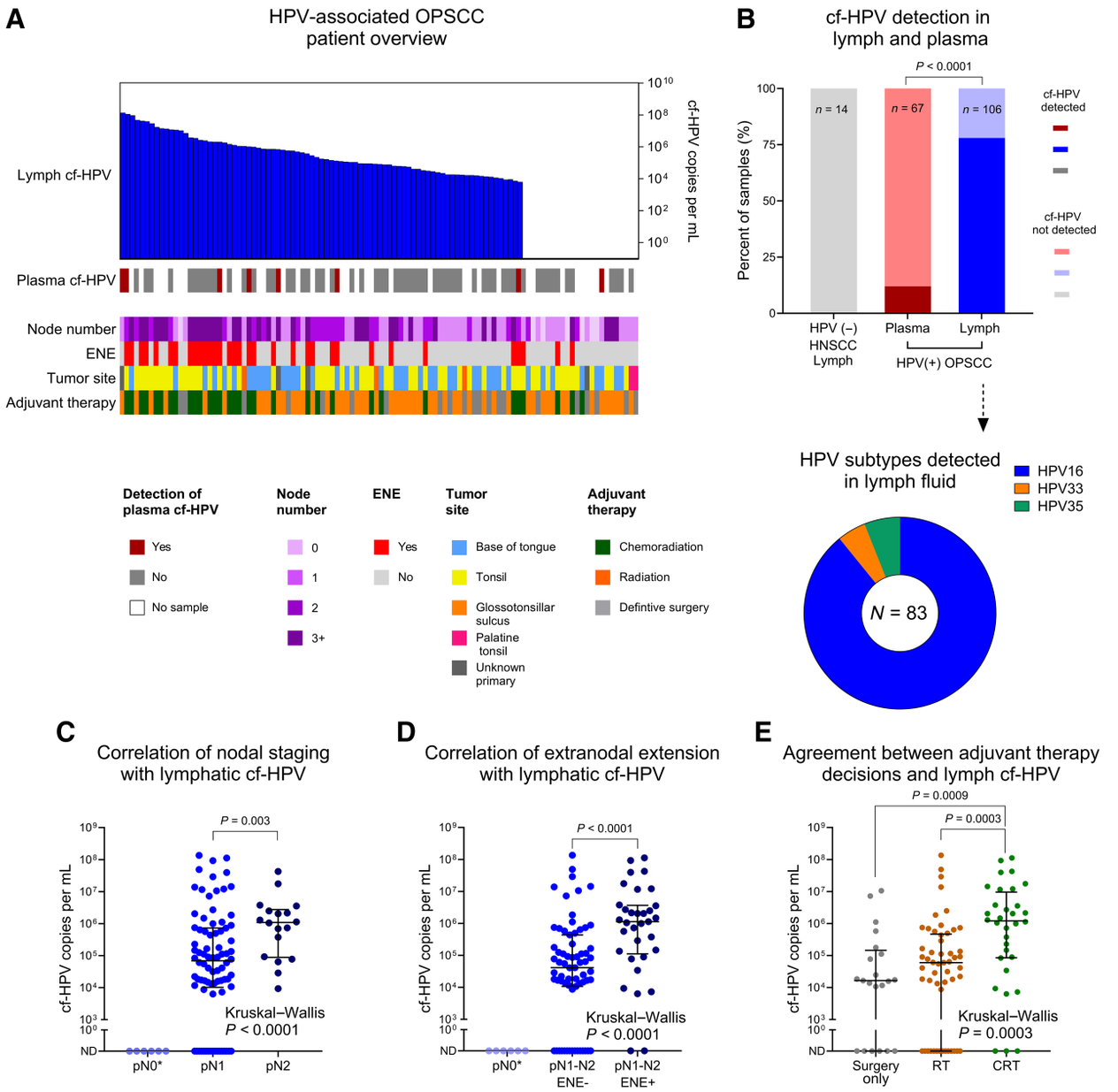

Figure 2.

Postoperative lymph from patients with HPV (+) OPSCC is enriched with cf-HPV, which correlates with nodal pathologic features. **A,** HPV (+) OPSCC cohort stratified by patient-level data: cf-HPV copies per mL in lymph, cf-HPV detection in plasma, number of involved lymph nodes, ENE, tumor site, and adjuvant treatment. **B,** 78% of lymph samples (83 of 106) from patients with HPV (+) OPSCC were cf-HPV (+) compared with 12% of paired plasma samples (8 of 67; $P < 0.0001$). The majority of lymph samples (74 of 83) and all plasma samples with detectable cf-HPV were HPV16 (+). Other high-risk subtypes detected in lymph included HPV33 (4 of 83) and HPV35 (5 of 83). **C,** Higher cf-HPV copies per ml in lymph were observed in patients with AJCC 8th edition nodal stage 2 (pN2) pathology than in those with pN1 disease ($P = 0.003$). **D,** A similar trend was observed in pN1-N2 patients with ENE compared with those without ENE ($P < 0.0001$). In addition, lymph from patients with no metastatic nodes identified during neck dissection (pN0*) lacked detectable cf-HPV (**C** and **D**). **E,** Lymph cf-HPV levels also reflected adjuvant treatment decision-making, as patients who received adjuvant CRT had a higher viral burden than those who received RT ($P = 0.0003$) or definitive surgery alone (Surgery only; $P = 0.0009$). Median and interquartile range are shown (**C**–**E**); cf-HPV detection differences were calculated using the Fisher exact test (**B**); pairwise cf-HPV copy number comparisons were assessed using the Mann–Whitney U test (**C**–**E**), and group comparisons were assessed using the Kruskal–Wallis test (**C**–**E**).

stage 2 (pN2) disease had more than 15-fold higher lymph cf-HPV (median = 1.09×10^6 copies/mL) than pN1 patients (median = 6.92×10^4 copies/mL; $P = 0.003$; **Fig. 2C**). In addition, patients with evidence of ENE had 27-fold higher cf-HPV (median = 1.13×10^6 copies/mL) than patients with positive nodes and no ENE (median = 4.14×10^4 copies/mL, $P < 0.0001$; **Fig. 2D**). These data suggest that cf-HPV levels in cervical lymph drain fluid after surgery reflect nodal disease burden.

We subsequently observed that cf-HPV correlated with other individual nodal pathologic risk features, including the number of positive nodes dissected at surgery (Spearman $\rho = 0.41$; $P < 0.0001$) and the ratio of positive nodes to total resected nodes (Spearman $\rho = 0.45$; $P < 0.0001$; Supplementary Fig. S4B). Crucially, we saw that patients with zero metastatic lymph nodes (pN0*) had no detectable cf-HPV signal (**Fig. 2C** and **D**). As pathology has a strong influence on postoperative adjuvant therapy escalation and lymph cf-HPV trends with more advanced nodal pathology, we classified our patients based on the adjuvant therapy that they subsequently received. We found that patients for whom our multidisciplinary tumor board offered CRT had significantly higher lymph cf-HPV levels than those who received RT ($P = 0.0003$) or definitive surgery alone ($P = 0.0009$; **Fig. 2E**). Interestingly, three patients treated with CRT had undetectable cf-HPV in their lymph; therefore, it is tempting to speculate that they could have had their treatment safely de-escalated.

Finally, because an extensive tobacco smoking history is strongly prognostic for inferior survival in HPV (+) disease (43), we investigated whether lymph cf-HPV was influenced by tobacco pack-years. We found no association between pack-years and higher lymph cf-HPV (Supplementary Fig. S4D and S4E). Taken together, these data show that cf-HPV after surgery is enriched in lymph relative to plasma, is specifically higher in patients with aggressive nodal pathologic features, and generally aligns with post-surgical adjuvant treatment decision-making by a multidisciplinary tumor board at a high-volume academic medical center.

Lymphatic fluid is enriched with tumor-informed ctDNA mutations

To complement our cf-HPV data, we also measured tumor-derived mutations in the lymphatic fluid. Thus, we conducted tumor-informed NGS on a subset of our HPV (+) lymph cohort patients ($N = 28$) using the Illumina TruSight Oncology 500 hybrid-capture panel (Supplementary Table S3). In 46% of lymph samples in this cohort (**Fig. 3A**), we identified nonsynonymous mutations in genes canonically associated with HPV (+) OPSCC in prior tumor sequencing studies (35–39). These included PI3K pathway (*PIK3CA* and *PTEN)*, DNA repair enzyme (*ATM* and *MSH2*), and chromatin stability (*KMT2C* and *EP300*) genes (Supplementary Table S4; Supplementary Table S5; **Fig. 3B**). In an additional 14% of lymph samples, we identified nonsynonymous mutations that are not typically associated with HPV (+) OPSCC (noncanonical mutations). Impressively, the burden of nonsynonymous mutations (**Fig. 3C**) and the median VAF (**Fig. 3D**) were both elevated in lymph samples from patients with pN2 ENE (+) nodal pathology compared with patients with either pN1 ENE (+) or pN0-N1 disease. These lymph mutational data overall reflect the findings observed in the lymph cf-HPV data (**Fig. 2C** and **D**).

Lymphatic cf-HPV reflects composite definitions of high-risk pathology

As no individual pathologic feature can fully account for high-risk disease, we stratified our patients according to four external definitions of high-risk pathology. These risk criteria were derived from four adjuvant treatment de-escalation clinical trials that enrolled only patients with HPV-associated OPSCC: Eastern Cooperative Oncology Group (ECOG) 3311 (22), MC 1273 (19), HPV-DART (20), and PATHOS (ref. 21; Supplementary Table S6). After applying all four classification criteria to our cohort, we observed that patients with trial-defined high-risk pathology consistently had elevated lymph cf-HPV compared with patients with either intermediate-risk disease (DART-HPV, MC 1273, PATHOS) or low-risk (ECOG 3311, PATHOS) pathology (Mean AUC = 0.78; **Fig. 4A** and **B**). Collectively, these data suggest that locoregional lymph cf-HPV can stratify patients according to multifeature definitions of pathologic risk.

Prognostic decision tree model incorporating lymph cfDNA stratifies outcomes

Lymph fluid is available immediately after surgery. Therefore, lymphatic cfDNA analysis can be performed in parallel with surgical pathology review. As our group has prior experience in generating prognostic machine learning models based on urine ctDNA MRD (27), we designed a proof-of-concept MRD risk model using a GBDT algorithm to perform binary classification (Supplementary Fig. S5A). The GBDT model integrated postoperative lymph and plasma cf-HPV with various clinicopathologic features (Supplementary Fig. S5B). Following 5-fold cross-validation, patients defined as high-risk by our postoperative MRD model (high-risk MRD) had significantly worse PFS than low-risk MRD patients (HR = 23; $P < 0.0001$; **Fig. 5A**). ROC analysis further demonstrated strong model performance for classifying relapse (AUC = 0.96; **Fig. 5B**), and lymph cf-HPV was the second-most important feature driving this performance (Supplementary Fig. S5B).

Lymph MRD can inform adjuvant treatment decision-making

To illustrate the practical utility of our lymph MRD assay to impact clinical care, we present two clinical vignettes that focus on two patients with pathologically low-risk disease. Patients 27 (**Fig. 5C**) and 102 (**Fig. 5D**) underwent TORS at our institution, which revealed p16 (+) stage pT1N1 primary tumors in both patients. Neither patient had positive surgical margins or evidence of ENE, and neither patient received adjuvant RT. One day after surgery, their plasma samples were cf-HPV MRD-negative, but both patients' postoperative lymph samples were cf-HPV MRD-positive. Eleven months later, Patient 27 suffered a locoregional recurrence in an ipsilateral cervical lymph node, while Patient 102 suffered locoregional relapse at 3 months, also in an ipsilateral cervical node (**Fig. 5C** and **D**). In both cases, postoperative cervical lymphatic cf-HPV detection was consistent with eventual relapse, whereas plasma cf-HPV was not.

Indeed, across all ten recurrences in our cohort, high-risk pathology, as defined by Bernier and colleagues (44), was only present in 50% of all cases and 25% of locoregional cases, while plasma cf-HPV was detectable in only 25% of all cases and 0% of locoregional cases. Conversely, lymph cf-HPV was detectable in all ten recurrence cases (Supplementary Fig. S6). These data further suggest that some patients with low-risk pathology and a high potential to be cured by definitive surgery alone, or some other form of treatment de-escalation, will still experience relapses that pathology alone cannot predict. While plasma cf-HPV detection lacked sensitivity immediately after surgery, locoregional MRD detection in the postoperative lymph appeared to capture disease relapse risk quite robustly and could be used as an adjunct to pathology in the future.

Discussion

Prior studies have demonstrated the utility of cf-HPV MRD detection in saliva and plasma of patients with HPV (+) OPSCC (11–15). Here, we expand upon this body of work by presenting the first prospective study demonstrating the efficacy of cf-HPV and ctDNA detection in cervical lymphatic drain fluid as proximal biomarkers for cancer-associated MRD detection early after neck dissection. Strikingly, we found that lymph contains significantly greater levels of cf-

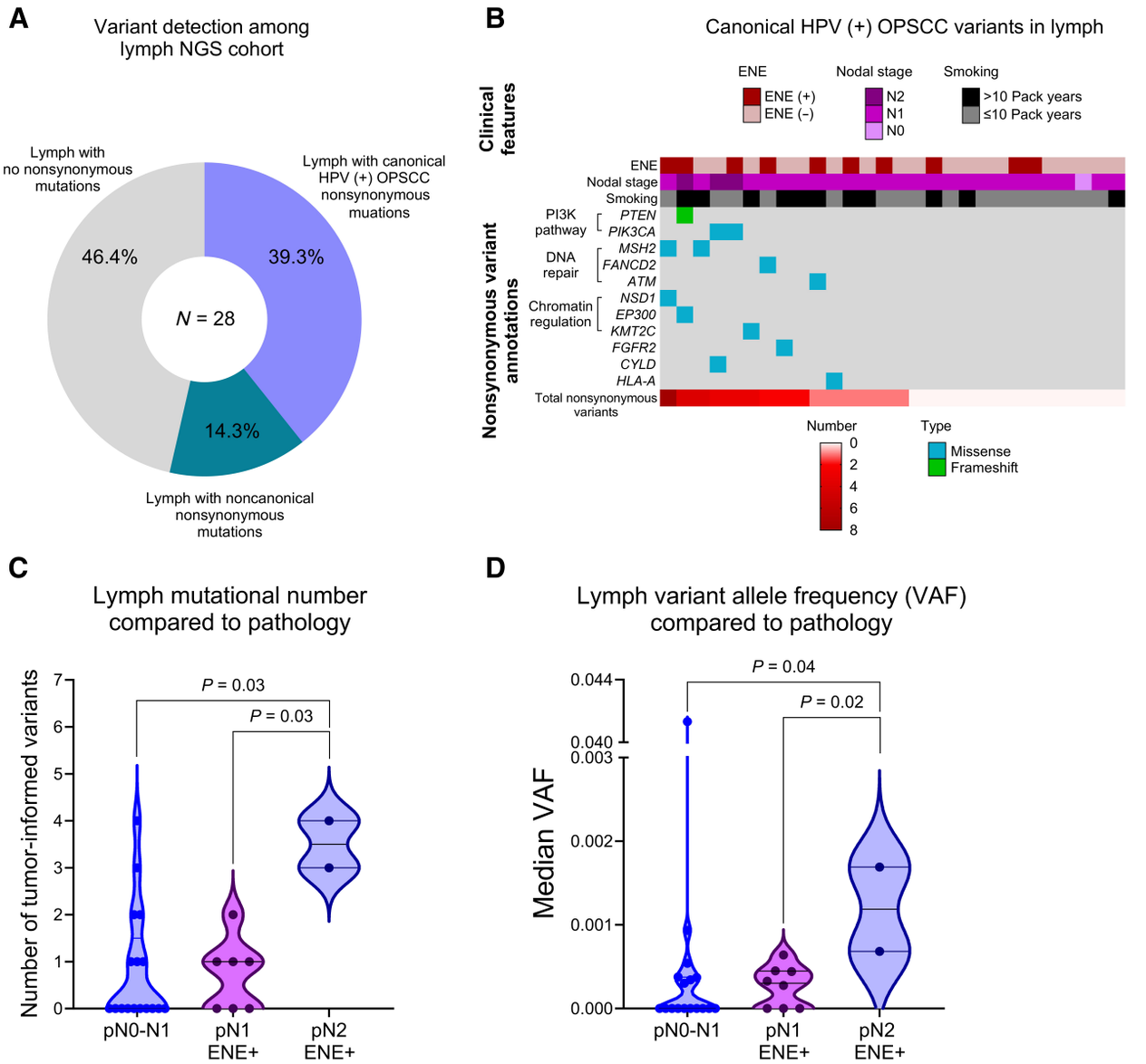

Figure 3.

Lymph cfDNA hybrid-capture sequencing revealed that the number of nonsynonymous tumor-informed variants increased with more aggressive pathology, similar to cf-HPV. **A,** Pie graph classifies all patients in the lymph NGS cohort ($N = 28$) according to tumor-informed variant detection and type: lymph containing at least one canonical HPV (+) OPSCC nonsynonymous mutation, lymph containing noncanonical nonsynonymous mutations, and lymph with no nonsynonymous mutations. Canonical genes were identified in prior HPV (+) OPSCC tumor sequencing studies (Materials and Methods). The heat map (**B**) annotates the specific genes in which canonical lymph variants occurred and the type of nonsynonymous mutation (missense or frameshift). It further displays patient-level clinical features: pathology (ENE status and pN stage), smoking history, and the total tumor-informed nonsynonymous mutational count (canonical and noncanonical). Next, the total number of nonsynonymous lymph ctDNA mutations (**C**) and the median lymph VAF (**D**) for each patient were stratified according to nodal pathology. **C,** Lymph from pN2 ENE (+) patients had more mutations than pN1 ENE (+) ($P = 0.03$) and pN0-N1 ENE (−) ($P = 0.03$) patients. **D,** Likewise, pN2 NE (+) patients had higher median lymph VAFs compared with pN1 ENE (+) ($P = 0.02$) and pN0-N1 ENE (−) ($P = 0.04$). Pairwise comparisons were performed using the Mann–Whitney U test (**C** and **D**).

HPV than plasma after surgery for HPV (+) head and neck cancer (**Fig. 2**; Supplementary Fig S4). This is in line with similar enrichment of cancer-associated cfDNA in urine in bladder cancer patients (27), with both urine and lymph drainage representing more proximal biofluids for cfDNA analysis than plasma.

We also compared lymph cf-HPV MRD with surgical pathology, the gold standard for adjuvant therapy decision making after surgery for HPV (+) OPSCC (19–22). As expected, primary tumor pathologic features were not associated with lymph cf-HPV, but nodal disease burden and ENE were (**Fig 2**; Supplementary Fig. S4). This demonstrates that viral burden in this proximal biofluid reflects the gold-standard pathologic hallmarks of disease burden and aggression in the cervical lymph nodes. We also observed higher lymph mutational burdens and variant allelic frequencies in patients with advanced nodal

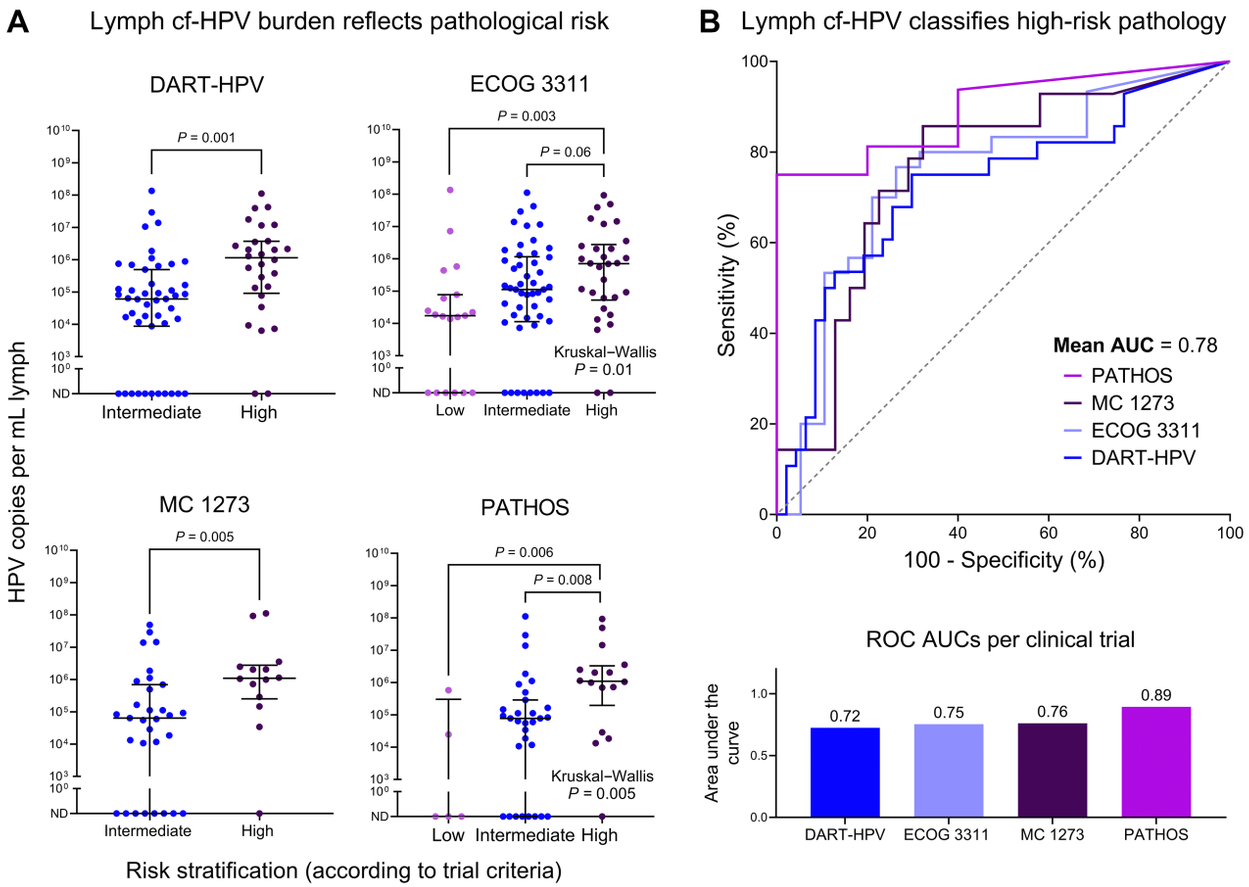

Figure 4.

Lymph cf-HPV MRD burden is strongly associated with composite definitions of high-risk pathology derived from four postoperative treatment de-escalation clinical trials carried out in patients with HPV (+) OPSCC. **A,** Lymph cf-HPV burden was elevated in high-risk patients compared with low- or intermediate-risk patients according to the classification criteria used in the DART-HPV (MC 1675) ($P = 0.001$), ECOG 3311 ($P = 0.01$), MC 1273 ($P = 0.005$), and PATHOS ($P = 0.005$) clinical trials. **B,** Receiver operating characteristic (ROC) curves were generated by comparing lymph cf-HPV between high- and low-risk patients (ECOG 3311 and PATHOS) or between high- and intermediate-risk patients (DART-HPV and MC 1273). The bar plot depicts area under the curve (AUC) (mean = 0.78). Pairwise comparisons were performed using the Mann–Whitney U test (**A**), and group comparisons were performed using the Kruskal–Wallis test (**A**).

pathology (**Fig. 2**; **Fig. 3**). This is exciting given that the mutational burden in HPV (+) OPSCC is relatively low (45) compared with tobacco-associated malignancies such as lung cancer (46). Indeed, we believe that residual lymph ctDNA and cf-HPV represent molecular evidence of persistent postoperative disease (3). Notably, we did not observe any correlation between pack-years and lymph cf-HPV MRD burden (Supplementary Fig. S4), despite reports showing that smoking reduces survival among patients with HPV (+) OPSCC (43). However, this is likely explained by our prior study on HPV(+) OPSCC, which showed that increased smoking history does not directly cause more extensive disease but rather results in the suppression of anti-tumor immune activation (47).

We further explored how well lymph cf-HPV aligns with composite pathologic risk definitions and patient outcomes. When we classified 106 HPV (+) patients according to the risk definitions derived from four recent surgical de-escalation clinical trials (19–22), we observed strong associations between lymph cf-HPV and high-risk pathology across all criteria applied (Mean AUC = 0.78; **Fig. 2**). Similarly, when we classified our patients by subsequent adjuvant treatment, we observed a significant trend toward more treatment escalation associated with higher lymph cf-HPV levels. Finally, using machine learning, we integrated lymph and plasma cf-HPV with clinicopathologic data to generate MRD-informed risk groups and demonstrated that patients with high-risk MRD had significantly worse PFS ($P < 0.0001$; AUC = 0.96; **Fig. 4**). Interestingly, lymph cf-HPV was the second most essential model feature following the number of lymph nodes resected (Supplementary Fig. S5). This further corroborates the potential clinical utility of our lymph liquid biopsy assay to stratify HPV (+) OPSCC patient outcomes as early as 24 hours after oncologic surgery.

Taken together, our findings indicate that our proximal lymph-based liquid biopsy approach could play a future role in adjuvant treatment decision making. Notably, some patients who received CRT had no detectable MRD in their lymph, so perhaps they could have had their adjuvant treatment safely de-escalated (**Fig. 2**). In addition, the integration of lymph and plasma cfDNA analyses in the early postoperative period may provide prognostic insights into the risk and localization of future recurrences (**Fig. 5**). In the future it will be interesting to also integrate lymph analysis with saliva (25, 48), a similarly proximal biofluid. Further, a recent study applying

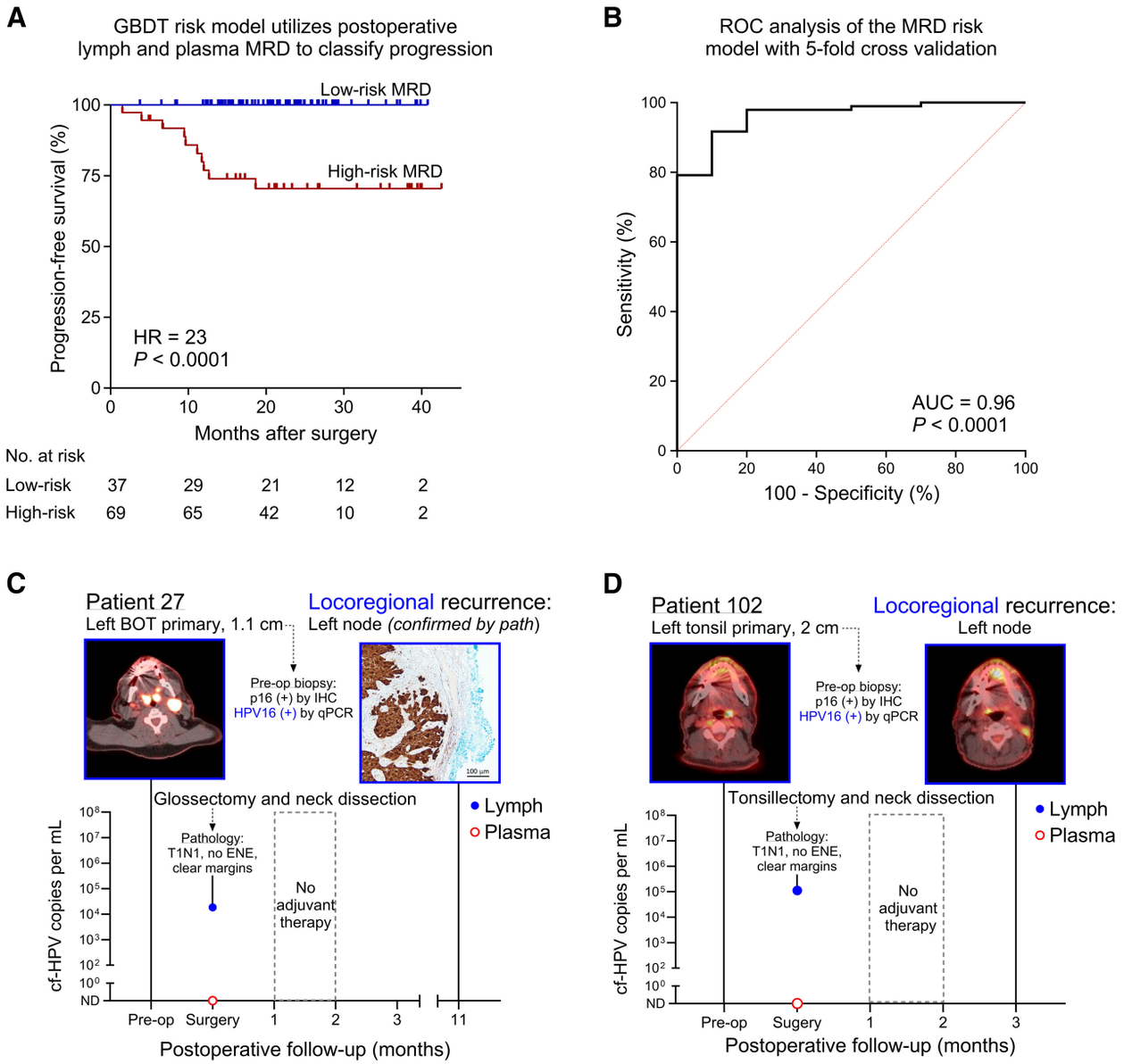

Figure 5.

Integration of lymph MRD, plasma MRD, and clinicopathologic data reflects the risk of disease relapse. **A,** A lymph-informed gradient-boosted decision tree (GBDT) model was trained and cross-validated for binary classification of patients with high- and low-risk disease based on clinicopathologic features and postoperative lymph and plasma MRD values (Materials and Methods). Kaplan–Meier PFS analysis was then performed according to risk status, which showed that high-risk patients had significantly worse outcomes (HR = 23; log-rank $P < 0.0001$). **B,** Receiver operating characteristic (ROC) curve for relapse versus no relapse classification shows strong model performance (AUC = 0.96) following 5-fold cross-validation. **C** and **D,** Clinical vignettes of 2 patients with low-risk disease (pT1N1, no evidence of ENE, and clear surgical margins) who were managed with surgery without adjuvant treatment. Postoperative plasma from both patients was MRD (−), but their lymph samples were MRD (+). In follow-up, Patient 27 (**C**) suffered locoregional relapse of cancer 11 months after surgery, while Patient 102 (**D**) developed locoregional recurrence 3 months after surgery, in both cases consistent with postoperative lymph MRD detection. BOT, base of tongue.

serial monitoring of plasma cf-HPV via ddPCR to patients with HPV (+) OPSCC treated with curative intent showed that although cf-HPV positive plasma samples had lead times on eventual relapse ranging from 97 to 166 days, plasma samples collected at 2 weeks posttreatment had low sensitivity to detect these recurrences (15). Thus, while plasma will remain crucial for long-term cancer surveillance, lymph could become instrumental for early prognostic insights available 24 hours after surgery. Following prospective assay validation in a larger cohort, a combined plasma and lymph assay could someday be used to assign patients to future de-escalation clinical trials (49) alongside surgical pathology (19–22). This ctDNA-informed approach has already shown success in de-escalating postoperative adjuvant therapy in stage II colorectal cancer (23). Indeed, going beyond head and neck cancer, numerous

resectable solid tumors spanning multiple disease sites (50–53) require surgical drain placement during the immediate postoperative period. Therefore, our tumor-informed lymph liquid biopsy approach could potentially be extended more broadly.

In summary, we demonstrated that lymph is a proximal bioanalyte that can facilitate locoregional MRD quantification, with higher lymph MRD being associated with increased risk of relapse after oncologic surgery for head and neck cancer. If these data can be further validated and extended, lymph could form the basis for a novel, rapid, practical, and sensitive method for personalized adjuvant treatment decision-making following surgery.

Limitations

Our study contained equivalent or higher HPV (+) OPSCC patient numbers compared with similar plasma cf-HPV studies (11–14), however, we had few recurrence events in line with expected treatment outcomes in HPV (+) disease (1, 2, 18). In addition, only five patients presented with pN0 disease at the time of surgery (Supplemental Methods). Therefore, it will be important to validate our assay's specificity in the pN0 setting and confirm if our lymph MRD informed machine learning approach can accurately predict relapse in a larger multi-institutional cohort. Despite these limitations, our assay showed significantly improved cf-HPV sensitivity compared with plasma, and that lymph cf-HPV levels correlated strongly with high-risk nodal pathology.

Authors' Disclosures

N.P. Semenkovich reports personal fees from Acuta Capital Management outside the submitted work. R.J. Ramirez reports a patent for US20230026377 with royalties paid from Washington University. Z. Gu reports personal fees from Droplet Biosciences, Inc. during the conduct of the study. B.M. Wahle reports a patent for "Surgical Drain for Collection and Preservation of Tumor-Associated Biomarkers in Surgical Drain Fluid"; it is listed under Wash U number 019650/WO-US pending, licensed, and with royalties paid from Washington University. W. Winckler reports personal fees from Droplet Biosciences outside the submitted work; in addition, W. Winckler has a patent for Unpublished filings in a related area pending and a patent for Unfiled IP in a related area pending. A.A. Chaudhuri reports other support from Droplet Biosciences during the conduct of the study as well as grants from Tempus Labs; other support from LiquidCell Dx and Geneoscopy; personal fees and nonfinancial support from Roche and Illumina; and personal fees from Myriad Genetics, Invitae, Daiichi Sankyo, AstraZeneca, DeciBio, Guidepoint, AlphaSights, Dava Oncology, and Agilent outside the submitted work; in addition, A.A. Chaudhuri has a patent for Systems and Methods for Integrated Analysis of Blood and Surgical Drain Fluid Biomarkers pending to Droplet Biosciences and a patent for Systems and Methods for Multimodal Analysis of Surgical Drain Fluid Using Interchangeable and Customizable Nucleic Acid Based Tests pending to Droplet Biosciences, NGS and analysis support from Droplet Biosciences, and ownership interests in Droplet Biosciences, and is on Droplet Bioscience's board of directors. J.P. Zevallos reports other support from Droplet Biosciences during the conduct of the study as well as other support from Vine Medical outside the submitted work; in addition, J.P. Zevallos has multiple patents related to surgical drain fluid as a diagnostic pending and with royalties paid. No disclosures were reported by the other authors.

Disclaimer

The funders had no role in study design, data collection and analysis, decision to publish, or preparation of the manuscript.

Authors' Contributions

N. Earland: Conceptualization, data curation, formal analysis, investigation, visualization, methodology, writing–original draft, writing–review and editing. **N.P. Semenkovich:** Software, formal analysis, methodology, writing–review and editing. **R.J. Ramirez:** Conceptualization, data curation, visualization, methodology, writing–review and editing. **S.P. Gerndt:** Data curation, investigation, methodology, writing–review and editing. **P.K. Harris:** Investigation, methodology, writing–review and editing. **Z. Gu:** Data curation, formal analysis, investigation, methodology, writing–review and editing. **A.I. Hearn:** Data curation, investigation, methodology, writing–review and editing. **M. Inkman:** Data curation, software, investigation, methodology, writing–review and editing. **J.J. Szymanski:** Investigation, methodology, writing–review and editing. **D. Whitfield:** Data curation, investigation, methodology, writing–review and editing. **B.M. Wahle:** Investigation, methodology, writing–review and editing. **Z. Xu:** Investigation, methodology, writing–review and editing. **K. Chen:** Investigation, methodology, writing–review and editing. **I. Alahi:** Formal analysis, investigation, methodology. **G. Ni:** Data curation, investigation, writing–review and editing. **A. Chen:** Data curation, methodology, writing–review and editing. **W. Winckler:** Formal analysis, investigation, methodology, writing–review and editing. **J. Zhang:** Investigation, methodology, writing–review and editing. **A.A. Chaudhuri:** Conceptualization, resources, supervision, funding acquisition, investigation, visualization, methodology, project administration, writing–review and editing. **J.P. Zevallos:** Conceptualization, resources, supervision, funding acquisition, investigation, visualization, methodology, project administration, writing–review and editing.

Acknowledgments

This work was supported by the Medical Scientist Training Program at the Washington University School of Medicine (to N. Earland); the National Institute of Deafness and Other Communication Disorders (NIDCD), through the "Development of Clinician/Researchers in Academic ENT" training grant, award number T32DC000022 (to R.J. Ramirez); the National Cancer Institute under award number U2C CA252981 (to A.A. Chaudhuri); the V Foundation V Scholar Award (to A.A. Chaudhuri); the Washington University Alvin J. Siteman Cancer Research Fund (to A.A. Chaudhuri); the Washington University Institute of Clinical and Translational Sciences grant UL1TR002345 from the National Center for Advancing Translational Sciences (NCATS; to J.P. Zevallos); and an R01 grant (CA211939) from the National Cancer Institute (to J.P. Zevallos).

Note

Supplementary data for this article are available at Clinical Cancer Research Online (http://clincancerres.aacrjournals.org/).

Received August 29, 2023; revised October 30, 2023; accepted November 3, 2023; published first November 8, 2023.

References

1. Cooper JS, Pajak TF, Forastiere AA, Jacobs J, Campbell BH, Saxman SB, et al. Postoperative concurrent radiotherapy and chemotherapy for high-risk squamous-cell carcinoma of the head and neck. N Engl J Med 2004;350:1937–44.
2. Bernier J, Domenge C, Ozsahin M, Matuszewska K, Lefèbvre J-L, Greiner RH, et al. Postoperative irradiation with or without concomitant chemotherapy for locally advanced head and neck cancer. N Engl J Med 2004;350:1945–52.
3. Pierik AS, Leemans CR, Brakenhoff RH. Resection margins in head and neck cancer surgery: an update of residual disease and field cancerization. Cancers 2021;13:2635.
4. Purandare NC, Puranik AD, Shah S, Agrawal A, Rangarajan V. Posttreatment appearances, pitfalls, and patterns of failure in head and neck cancer on FDG PET/CT imaging. Indian J Nucl Med 2014;29:151–7.
5. Moding EJ, Nabet BY, Alizadeh AA, Diehn M. Detecting liquid remnants of solid tumors: circulating tumor DNA minimal residual disease. Cancer Discov 2021;11:2968–86.
6. Semenkovich NP, Szymanski JJ, Earland N, Chauhan PS, Pellini B, Chaudhuri AA. Genomic approaches to cancer and minimal residual disease detection using circulating tumor DNA. J Immunother Cancer 2023;11:e006284.
7. Earland N, Chen K, Semenkovich NP, Chauhan PS, Zevallos JP, Chaudhuri AA. Emerging roles of circulating tumor DNA for increased precision and personalization in radiation oncology. Semin Radiat Oncol 2023;33:262–78.
8. Palmirotta R, Lovero D, Cafforio P, Felici C, Mannavola F, Pellè E, et al. Liquid biopsy of cancer: a multimodal diagnostic tool in clinical oncology. Ther Adv Med Oncol 2018;10:1758835918794630.

9. Wuerdemann N, Jain R, Adams A, Speel E-JM, Wagner S, Joosse SA, et al. Cell-free HPV-DNA as a biomarker for oropharyngeal squamous cell carcinoma: a step towards personalized medicine? Cancers 2020;12:2997.
10. Flach S, Howarth K, Hackinger S, Pipinikas C, Ellis P, McLay K, et al. Liquid BIOpsy for MiNimal RESidual DiSease detection in head and neck squamous cell carcinoma (LIONESS): a personalized circulating tumor DNA analysis in head and neck squamous cell carcinoma. Br J Cancer 2022;126:1186–95.
11. Chera BS, Kumar S, Beaty BT, Marron D, Jefferys S, Green R, et al. Rapid Clearance profile of plasma circulating tumor HPV Type 16 DNA during chemoradiotherapy correlates with disease control in HPV-associated oropharyngeal cancer. Clin Cancer Res 2019;25:4682–90.
12. Haring CT, Bhambhani C, Brummel C, Jewell B, Bellile E, Heft Neal ME, et al. Human papilloma virus circulating tumor DNA assay predicts treatment response in recurrent/metastatic head and neck squamous cell carcinoma. Oncotarget 2021;12:1214–29.
13. Routman DM, Kumar S, Chera BS, Jethwa KR, Van Abel KM, Frechette K, et al. Detectable postoperative circulating tumor human papillomavirus DNA and association with recurrence in patients with HPV-associated oropharyngeal squamous cell carcinoma. Int J Radiat Oncol Biol Phys 2022;113:530–8.
14. Fakhry C, Blackford AL, Neuner G, Xiao W, Jiang B, Agrawal A, et al. Association of oral human papillomavirus DNA persistence with cancer progression after primary treatment for oral cavity and oropharyngeal squamous cell carcinoma. JAMA Oncol 2019;5:985–92.
15. Jakobsen KK, Bendtsen SK, Pallisgaard N, Friborg J, Lelkaitis G, Grønhøj C, et al. Liquid biopsies with circulating plasma HPV-DNA measurements - a clinically applicable surveillance tool for HPV-positive oropharyngeal cancer patients. Clin Cancer Res 2023;29:3914–23.
16. Economopoulou P, Koutsodontis G, Avgeris M, Strati A, Kroupis C, Pateras I, et al. HPV16 E6/E7 expression in circulating tumor cells in oropharyngeal squamous cell cancers: a pilot study. PLoS One 2019;14:e0215984.
17. Marur S, D'Souza G, Westra WH, Forastiere AA. HPV-associated head and neck cancer: a virus-related cancer epidemic. Lancet Oncol 2010;11:781–9.
18. Fakhry C, Westra WH, Li S, Cmelak A, Ridge JA, Pinto H, et al. Improved survival of patients with human papillomavirus-positive head and neck squamous cell carcinoma in a prospective clinical trial. J Natl Cancer Inst 2008;100:261–9.
19. Ma DJ, Price K, Eric MJ, Patel SH, Hinni ML, Ginos BF, et al. Long-term results for MC1273, A Phase II evaluation of De-Escalated adjuvant radiation therapy for human papillomavirus associated oropharyngeal squamous cell carcinoma (HPV+ OPSCC). Int J Radiat Oncol Biol Phys 2021;111:S61.
20. Ma DM, Price K, Moore EJ, Patel SH, Hinni ML, Fruth B, et al. MC1675, a Phase III evaluation of De-Escalated adjuvant radiation therapy (DART) vs. standard adjuvant treatment for human papillomavirus associated oropharyngeal squamous cell carcinoma. Int J Radiat Oncol Biol Phys 2021;111:1324.
21. Evans M, Knott S, Hurt C, Patterson J, Robinson M, Hutcheson KA, et al. PATHOS: A phase II/III trial of risk-stratified, reduced intensity adjuvant treatment in patients undergoing transoral surgery for human papillomavirus (HPV)-positive oropharyngeal cancer. J Clin Orthod 2018;36:TPS6097.
22. Ferris RL, Flamand Y, Weinstein GS, Li S, Quon H, Mehra R, et al. Phase II randomized trial of transoral surgery and low-dose intensity modulated radiation therapy in resectable p16+ locally advanced oropharynx cancer: an ECOG-ACRIN cancer research group trial (E3311). J Clin Oncol 2022;40:138–49.
23. Tie J, Cohen JD, Lahouel K, Lo SN, Wang Y, Kosmider S, et al. Circulating tumor DNA analysis guiding adjuvant therapy in stage II colon cancer. N Engl J Med 2022;386:2261–72.
24. Corcoran RB, Chabner BA. Application of cell-free DNA analysis to cancer treatment. N Engl J Med 2018;379:1754–65.
25. Hanna GJ, Lau CJ, Mahmood U, Supplee JG, Mogili AR, Haddad RI, et al. Salivary HPV DNA informs locoregional disease status in advanced HPV-associated oropharyngeal cancer. Oral Oncol 2019;95:120–6.
26. Nair VS, Hui AB-Y, Chabon JJ, Esfahani MS, Stehr H, Nabet BY, et al. Genomic profiling of bronchoalveolar lavage fluid in lung cancer. Cancer Res 2022;82:2838–47.
27. Chauhan PS, Shiang A, Alahi I, Sundby RT, Feng W, Gungoren B, et al. Urine cell-free DNA multi-omics to detect MRD and predict survival in bladder cancer patients. NPJ Precis Oncol 2023;7:6.
28. Chauhan PS, Chen K, Babbra RK, Feng W, Pejovic N, Nallicheri A, et al. Urine tumor DNA detection of minimal residual disease in muscle-invasive bladder cancer treated with curative-intent radical cystectomy: A cohort study. PLoS Med 2021;18:e1003732.
29. Crosbie PAJ, Shah R, Krysiak P, Zhou C, Morris K, Tugwood J, et al. Circulating tumor cells detected in the tumor-draining pulmonary vein are associated with disease recurrence after surgical resection of NSCLC. J Thorac Oncol 2016;11:1793–7.
30. Doll C, Steffen C, Beck-Broichsitter B, Richter M, Neumann K, Pohrt A, et al. The prognostic significance of p16 and its role as a surrogate marker for human papilloma virus in oral squamous cell carcinoma: an analysis of 281 cases. Anticancer Res 2022;42:2405–13.
31. Randén-Brady R, Carpén T, Jouhi L, Syrjänen S, Haglund C, Tarkkanen J, et al. *In situ* hybridization for high-risk HPV E6/E7 mRNA is a superior method for detecting transcriptionally active HPV in oropharyngeal cancer. Hum Pathol 2019;90:97–105.
32. Surgery Followed by Risk-Directed Post-Operative Adjuvant Therapy for HPV-Related Oropharynx Squamous Cell Carcinoma: "The Minimalist Trial (MINT)" - Full Text View - ClinicalTrials.gov. Available from: https://www.clinicaltrials.gov/ct2/show/NCT03621696
33. Forootan A, Sjöback R, Björkman J, Sjögreen B, Linz L, Kubista M. Methods to determine limit of detection and limit of quantification in quantitative real-time PCR (qPCR). Biomol Detect Quantif 2017;12:1–6.
34. Abbosh C, Swanton C, Birkbak NJ. Clonal hematopoiesis: a source of biological noise in cell-free DNA analyses. Ann Oncol 2019;30:358–9.
35. Haft S, Ren S, Xu G, Mark A, Fisch K, Guo TW, et al. Mutation of chromatin regulators and focal hotspot alterations characterize human papillomavirus-positive oropharyngeal squamous cell carcinoma. Cancer 2019;125:2423–34.
36. Pan C, Issaeva N, Yarbrough WG. HPV-driven oropharyngeal cancer: current knowledge of molecular biology and mechanisms of carcinogenesis. Cancers Head Neck 2018;3:12.
37. Giudice FS, Squarize CH. The determinants of head and neck cancer: Unmasking the PI3K pathway mutations. J Carcinog Mutagen 2013;Suppl 5:003.
38. Stransky N, Egloff AM, Tward AD, Kostic AD, Cibulskis K, Sivachenko A, et al. The mutational landscape of head and neck squamous cell carcinoma. Science 2011;333:1157–60.
39. Seiwert TY, Zuo Z, Keck MK, Khattri A, Pedamallu CS, Stricker T, et al. Integrative and comparative genomic analysis of HPV-positive and HPV-negative head and neck squamous cell carcinomas. Clin Cancer Res 2015;21:632–41.
40. TabularPredictor.Feature_importance. AutoGluon. Available from: https://auto.gluon.ai/stable/api/autogluon.tabular.TabularPredictor.feature_importance.html
41. Xue X, Agalliu I, Kim MY, Wang T, Lin J, Ghavamian R, et al. New methods for estimating follow-up rates in cohort studies. BMC Med Res Methodol 2017;17:155.
42. Mazul AL, Rodriguez-Ormaza N, Taylor JM, Desai DD, Brennan P, Anantharaman D, et al. Prognostic significance of non-HPV16 genotypes in oropharyngeal squamous cell carcinoma. Oral Oncol 2016;61:98–103.
43. Ang KK, Harris J, Wheeler R, Weber R, Rosenthal DI, Nguyen-Tân PF, et al. Human papillomavirus and survival of patients with oropharyngeal cancer. N Engl J Med 2010;363:24–35.
44. Bernier J, Cooper JS, Pajak TF, van Glabbeke M, Bourhis J, Forastiere A, et al. Defining risk levels in locally advanced head and neck cancers: a comparative analysis of concurrent postoperative radiation plus chemotherapy trials of the EORTC (#22931) and RTOG (# 9501). Head Neck 2005;27:843–50.
45. Xu S-M, Shi C-J, Xia R-H, Wang L-Z, Tian Z, Ye W-M, et al. Analysis of immunological characteristics and genomic alterations in HPV-positive oropharyngeal squamous cell carcinoma based on PD-L1 expression. Front Immunol 2021;12:798424.
46. Ramos-Paradas J, Hernández-Prieto S, Lora D, Sanchez E, Rosado A, Caniego-Casas T, et al. Tumor mutational burden assessment in non-small-cell lung cancer samples: results from the TMB2 harmonization project comparing three NGS panels. J Immunother Cancer 2021;9:e001904.
47. Wahle BM, Zolkind P, Ramirez RJ, Skidmore ZL, Anderson SR, Mazul A, et al. Integrative genomic analysis reveals low T-cell infiltration as the primary feature of tobacco use in HPV-positive oropharyngeal cancer. iScience 2022;25:104216.
48. Wasserman JK, Rourke R, Purgina B, Caulley L, Dimitroulakos J, Corsten M, et al. HPV DNA in saliva from patients with SCC of the head and neck is specific for p16-positive oropharyngeal tumors. J Otolaryngol Head Neck Surg 2017;46:3.
49. Haring CT, Dermody SM, Yalamanchi P, Kang SY, Old MO, Chad Brenner J, et al. The future of circulating tumor DNA as a biomarker in HPV

related oropharyngeal squamous cell carcinoma. Oral Oncol 2022;126: 105776.
50. Villafane-Ferriol N, Shah RM, Mohammed S, Van Buren G 2nd, Barakat O, Massarweh NN, et al. Evidence-based management of drains following pancreatic resection: a systematic review. Pancreas 2018;47:12–7.
51. Samaiya A. To drain or not to drain after colorectal cancer surgery. Indian J Surg 2015;77:1363–8.
52. Weindelmayer J, Mengardo V, Veltri A, Baiocchi GL, Giacopuzzi S, Verlato G, et al. Utility of abdominal drain in gastrectomy (ADiGe) trial: study protocol for a multicenter non-inferiority randomized trial. Trials 2021;22: 152.
53. Kalogera E, Dowdy SC, Mariani A, Aletti G, Bakkum-Gamez JN, Cliby WA. Utility of closed suction pelvic drains at time of large bowel resection for ovarian cancer. Gynecol Oncol 2012;126:391–6.